ChemPubSoc Europe

DOI: 10.1002/ejic.201601329

EurJIC European Journal of Inorganic Chemistry

Full Paper

Nitrosyl Complexes | *Very Important Paper* |

Structure and Bonding of High-Spin Nitrosyl–Iron(II) Compounds with Mixed N,O-Chelators and Aqua Ligands

Markus Wolf[a] and Peter Klüfers*[a]

Dedicated to Professor Wolfgang Beck on the occasion of his 85th birthday

Abstract: High-spin nitrosyl–iron centres of the Enemark–Feltham {FeNO}^{7} type exist in aqueous solution. Examples include the tentative "brown-ring" species $[Fe(H_2O)_5(NO)]^{2+}$ and a tentative Fe^{II}/edta/NO species formed in the processes for scrubbing NO from flue-gas streams. Inert-gas bubbling through the solutions subdivides the ferrous nitrosyl complexes in a less stable subclass – a prominent member being the brown-ring complex – and a more stable subclass to which the edta species belongs. The structural chemistry of the less stable subclass of {FeNO}^{7}-type complexes from aqueous media is presented here. They contain aminecarboxylato co-ligands of limited denticity and aqua ligands that complete an *OC*-6 environment of the Fe atom. Crystalline compounds for single-crystal structure analysis were obtained for various co-ligands: $[Fe(H_2O)_2(ida)(NO)]$ (**2a**), $[Fe(H_2O)(heida)(NO)]$ (**2b**), $[Fe(H_2O)_2(NO)(oda)]$ (**2c**), $[Fe(H_2O)_2(NO)(phida)]\cdot H_2O$ (**2d**), $[Fe(bnida)(H_2O)_2(NO)]$ (**2e**), $[Fe(brbnida)(H_2O)_2(NO)]$ (**2f**) and $[Fe(dipic)(H_2O)_2(NO)]$ (**2g**) (ida = iminodiacetate, heida = hydroxyethyliminodiacetate, oda = oxodiacetate, phida = *N*-phenyliminodiacetate, bnida = *N*-benzyliminodiacetate, brbnida = *N*-4-bromobenzyliminodiacetate, dipic = dipicolinate). The Fe–NO interaction was studied by DFT and CASSCF methods. Due to mostly covalent Fe–NO π bonds, the charge distribution in the less stable subclass is close to $Fe^{II}(NO)$ with a small $Fe^{III}(NO^-)$ contribution.

Introduction

There are few scientific topics that have attracted unweaning interest for more than a century. The structure and the bonding situation of adducts of high-spin iron(II) with nitric oxide is one of them.

In a first period of intense research, the focus was laid on aqua–Fe(NO) or halogenido–Fe(NO) species, which were prepared by the reaction of nitric oxide gas and ferrous salts dissolved in diluted aqueous acids or concentrated hydrochloric acid, respectively.[1] The motivation to conduct such experiments was the attempt to isolate the chromophore of the tentative nitrosyl–iron species in nitrate ("brown-ring test") and nitrite detection. After about a decade of mere data collection, first attempts were made to assign formulae to the iron–nitrosyl species. Thus, the brown species formed in neutral to weakly acidic solutions was assigned the formula $Fe(NO)^{2+}$, and the related green species from the reaction of ferrous chloride and NO in concentrated hydrochloric acid was formulated as $[FeCl_{2+x}(NO)]^{x-}$ by Kohlschütter, who was one of the first who adapted Werner's concept of coordination compounds (the charges were deduced from transference experiments). A characteristic of this early research has remained a constant feature, namely the hesitation of the species to form crystalline salts. Even the parent species of this chemistry, the aquated $Fe(NO)^{2+}$ cation, has never been isolated as a crystalline salt in a reproducible way (Wilkinson reported "rather ill-defined solids" on his attempts to reproduce crystals claimed by Manchot to contain this cation).[1d,2] It should be noted in this context that all researchers mentioned the limited stability of the tentative $Fe(NO)^{2+}(aq)$ species, which is not shared, for example, by the chlorido derivatives.

Later, further milestones were reached. About 90 years ago, UV/Vis spectra – badly resolved due to the limitations of the available apparatuses – showing the spectral features of the $Fe^{II}(NO)$ chromophore were published.[3] The generally accepted formulation of the aquated dication as an octahedral $[Fe(H_2O)_5(NO)]^{2+}$ species was proposed in a 1958 work by Griffith, Lewis and Wilkinson. Their argument for assuming solely aqua co-ligands was based on the chromophore's formation in the absence of anions of coordination ability stronger than perchlorate. Moreover, they conducted magnetic measurements to show the $S = 3/2$ spin state of this species, which they interpreted as a high-spin d^7-iron(I) complex with an NO^+ ligand.[2] Some 40 years ago, when coordination chemistry was focused on organometallic approaches, species such as the green $[FeCl_3(NO)]^-$ were isolated (though not in crystals) after the reaction of the low-valent, low-spin iron precursor $[Fe(CO)_3(NO)]^-$ with elemental chlorine. EPR- and IR-spectroscopic data of the trichlorido species, which was still seen as an $Fe^I(NO^+)$ species, were reported.[4] The influential review on metal–nitrosyl complexes by Enemark and Feltham fell into this

[a] *Department Chemie, Ludwig-Maximilians-Universität München, Butenandtstraße 5-13, 82377 München, Germany*
E-mail: kluef@cup.uni-muenchen.de
http://www.cup.lmu.de/ac/kluefers/homepage/

Supporting information for this article is available on the WWW under http://dx.doi.org/10.1002/ejic.201601329.

period.[5] In their nomenclature, they avoided the ambiguous oxidation-state assignment and classified nitrosyl–metal complexes by simply summing up the metal d and the NO -π* electrons. The species in question here belong thus to the {FeNO}^{7} class [d^7 + $(\pi^*)^0$], [d^6 + $(\pi^*)^1$] or [d^5 + $(\pi^*)^2$], depending on the formulation of $Fe^{I}(NO^+)$, $Fe^{II}(NO)$ or $Fe^{III}(NO^-)$ couples. More specifically, we are dealing with the {FeNO}^{7}(S = 3/2) subclass here. Another subclass that is not addressed comprises the related low-spin {FeNO}^{7}(S = 1/2) species, which are found with porphyrin and related co-ligands. The same holds for tetrahedral {FeNO}^{7}(S = 3/2) centres, which, comprising mostly thiolate co-ligands, have evolved into a vivid branch of biochemically motivated investigations on the chemistry of the small hormone NO.[6]

In the 1980s, aminecarboxylates were introduced into the field of {FeNO}^{7}(S = 3/2) complexes, motivated by the idea of using the enhanced Fe^{II}–NO binding by aminecarboxylato co-ligands for the development of agents suitable for the removal of NO from power-plant flue-gas streams.[7] The data collected in this period indicated that the stability of the Fe^{II}–NO bond follows the stability of the NO-free iron(II)/aminecarboxylate complex. Two decades later, the body of spectroscopic, kinetic and thermodynamic data on aqueous solutions of aminecarboxylate-supported ferrous nitrosyl compounds was completed comprehensively in a series of publications by the van Eldik group.[8] The authors state that a higher stability of the Fe–NO linkage in the presence of multidentate aminecarboxylate co-ligands is correlated with a higher trivalent character of the central atom.

Prior to these latter systematic investigations, the Solomon group used the Fe/edta/NO complex as a reference species to re-evaluate the bonding characteristics of the quartet-{FeNO}^{7} state.[9] The experimental basis for their computational approach included a variety of methods such as X-ray absorption, resonance Raman, UV/Vis absorption, magnetic circular dichroism and electron paramagnetic resonance spectroscopy as well as SQUID magnetic susceptibility data. However, a particularly significant method, X-ray crystallography, was unavailable. Solomon's computational analysis resulted in a re-formulation of the quartet-{FeNO}^{7} bonding situation as a high-spin ferric centre (S = 5/2), antiferromagnetically coupled to a triplet NO^- ligand (S = 1), that is, to NO^- in its electronic ground state (note the isoelectronic relationship to O_2), resulting in the observed quartet state. In the context of these investigations, a re-interpretation of the parent quartet-$[Fe(H_2O)_5(NO)]^{2+}$ species was undertaken by several groups. The analysis of the electronic structure depended on the theoretical level and resulted in assignments between a high-spin $[Fe^{III}(H_2O)_5(^3NO^-)]^{2+}$ and a high-spin $[Fe^{II}(H_2O)_5(NO)]^{2+}$ bonding situation, with preference for the latter.[6,10]

The lack of structural data for the Fe/edta/NO species has been mentioned. An odd situation arises when laying the focus on octahedral quartet-{FeNO}^{7} species. Despite the fact that, currently, about two dozen single-crystal analyses of this class of species are available (a compilation is presented in the Supporting Information, also see ref.[11]), no species has been crystallised from an aqueous solution. Accordingly, no crystal structure is available that shows aqua co-ligands. The significance of both aspects – the isolation of hydrolytically stable quartet-{FeNO}^{7} species and the concomitant presence of aqua and nitrosyl ligands – is highlighted by current publications on this topic. The first aspect has remained a matter of interest for three decades, namely the use of aqueous Fe/edta solutions as NO absorbents. Thus, in recent processes, nitric oxide scrubbing cycles were combined with biological reductants.[9c] With regard to the second aspect, the lack of structural data is nicely demonstrated in attempts to model the so-called facial triad (two histidine and one carboxylate ligands) of mononuclear non-heme iron oxygenases by aminecarboxylate ligands. In a recent work, advanced EPR technology was used to elucidate the structure of both (!) the enzyme's active site and the aminecarboxylate–aqua-{FeNO}^{7} model compounds due to the lack of structural data also for the latter.[12]

The aim of this and the accompanying publication[13] is to increase the knowledge of the structural chemistry of octahedrally coordinated quartet-{FeNO}^{7} centres. To properly organise the experimental and computational results, the above-mentioned stability criterion was used. In this first part, we restrict ourselves to co-ligands that lead to aqueous solutions of limited NO-binding capability as detected by simply bubbling an inert gas such as argon through the respective solution. All solutions described in this work lose nitric oxide during this procedure. Hence, the dark-greenish {FeNO}^{7} centres turn to almost colourless co-ligand–iron(II) complexes in the course of the experiment. With respect to this test, stable solutions are the focus of the accompanying publication.[13]

Scheme 1 illustrates the different co-ligands **1** that we used in this work. They are all derived from iminodiacetic acid (H_2ida, **1a**), whose dianion is a potentially tridentate chelator.

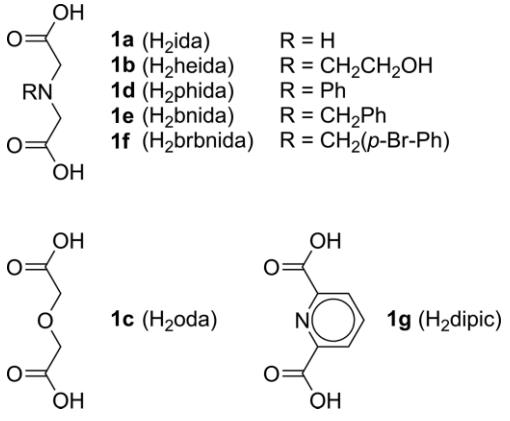

Scheme 1. The dibasic parent acids of the chelating ligands used for the synthesis of the quartet-{FeNO}^{7} compounds in this work.

Results and Discussion

Scheme 2 displays the synthetic route employed for the preparation of the quartet-{FeNO}^{7} compounds: $FeSO_4$ reacts in aqueous solution with nitric oxide and one equivalent of iminodiacetic acid (**1a**) or its derivatives (**1b**–**1g**) to yield dark-green solutions of **2**. Under inert-gas conditions, these solutions are

stable for several months at room temperature. In contact with air, they decompose within several hours. When low pressure or heat is applied, or when the solutions are purged with argon or nitrogen, they lose nitric oxide quite rapidly. By the diffusion of acetone into the solutions, we obtained black-green crystals of **2**, suitable for X-ray diffraction analyses. The solid compounds are stable against oxygen and moisture. They cannot be re-dissolved in common solvents and start to decompose at temperatures of about 150 °C. Crystals of **2a** demonstrated that irradiation does not result in the loss of nitric oxide as observed for the aqueous solutions. Remarkably, UV irradiation resulted in the decarboxylation of the ida ligand, as detected by the CO_2 absorption band in the IR spectrum of the irradiated crystals.[14]

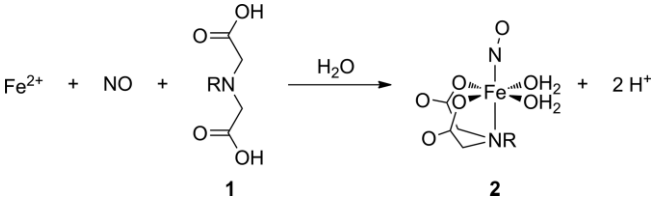

Scheme 2. Procedure for the synthesis of the quartet-{FeNO}^{7} compounds **2**.

X-ray Diffraction

Crystal-structure determination revealed the octahedral coordination of the iron central atom for all compounds **2**. The chelating ligands coordinate either facially, as in compounds **2a**, **2b**, **2e** and **2f** (see Figures 1 and 2 for **2a** and **2b**, respectively), or meridionally, as in compounds **2c**, **2d** and **2g** (see Figures 3, 4 and 5, respectively). Nitric oxide coordinates in a slightly bent fashion *trans* to the central heteroatom of the chelate ligand (except in **2d**). The remaining positions are occupied by aqua ligands, which support a three-dimensional hydrogen-bond network that connects the complex units. With Fe–N_{NO} distances between 1.76 and 1.80 Å, N–O distances between 1.09 and 1.17 Å and Fe–N–O angles between 148 and 171° (Table 1), compounds **2** match the crystalline quartet-{FeNO}^{7} compounds with octahedral coordination, known in the literature.[15] Besides these similarities, compounds **2** are unique as they are the first crystalline {FeNO}^{7} compounds with aqua ligands. Figure 6 shows compound **3g**, the nitrosyl-free homologue of **2g**.

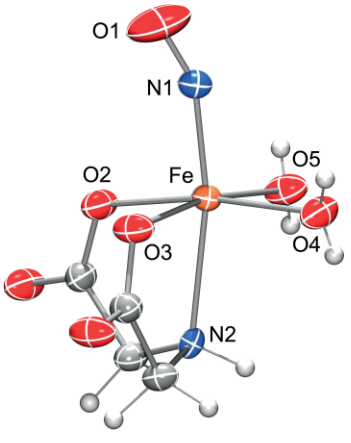

Figure 1. [Fe(H_2O)$_2$(ida)(NO)] molecules in crystals of **2a**. Space group: *Cmc*2$_1$. Thermal ellipsoids are drawn at 50 % probability.

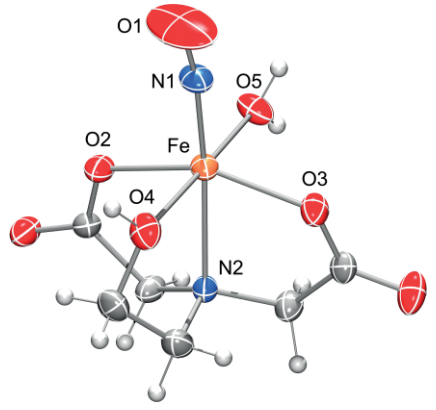

Figure 2. [Fe(H_2O)(heida)(NO)] molecules in crystals of **2b**. Space group: *Cc*. Thermal ellipsoids are drawn at 50 % probability.

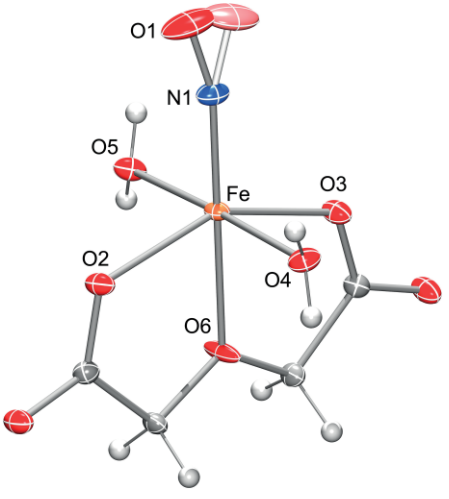

Figure 3. [Fe(H_2O)$_2$(NO)(oda)] molecules in crystals of **2c**. Space group: *Aba*2. Thermal ellipsoids are drawn at 50 % probability. O1 is disordered.

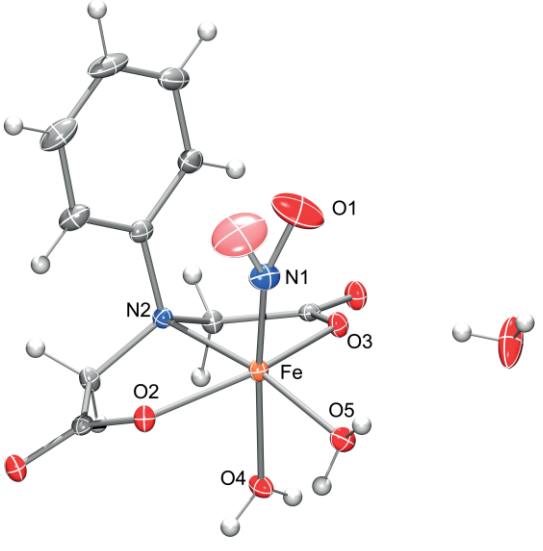

Figure 4. [Fe(H_2O)$_2$(NO)(phida)]·H_2O moieties in crystals of **2d**. Space group: *Pbca*. Thermal ellipsoids are drawn at 50 % probability. O1 is disordered.

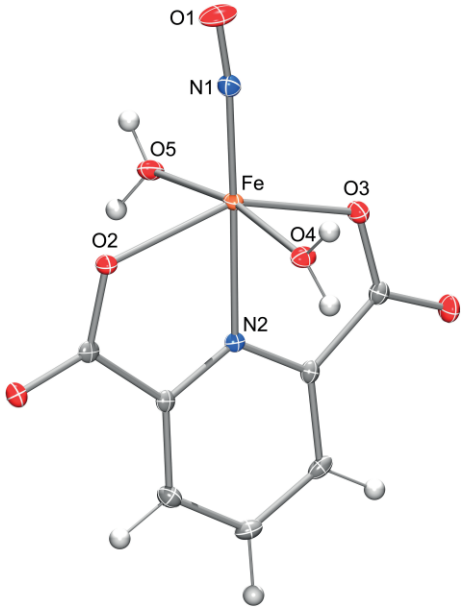

Figure 5. [Fe(dipic)$(H_2O)_2$(NO)] molecules in crystals of **2g**. Space group: $P2_12_12_1$. Thermal ellipsoids are drawn at 50 % probability.

Table 1. Bond lengths (in Å) and angles (in °) in compounds **2**.

	2a	**2b**	**2c**	**2d**	**2e**	**2f**	**2g**	**3g**
Fe–N1/O7	1.78	1.76	1.77	1.78	1.78	1.80	1.76	2.06
N1–O1	1.11	1.11	1.15	1.17	1.13	1.09	1.14	–
Fe–N1–O1	155	171	165	148	165	158	167	–
Fe–O2	2.05	2.05	2.07	2.03	2.07	2.05	2.14	2.17
Fe–O3	2.05	2.05	2.07	2.02	2.06	2.04	2.10	2.16
Fe–O4	2.06	2.10	2.08	2.19	2.06	2.06	2.11	2.11
Fe–O5	2.06	2.08	2.08	2.02	2.04	2.04	2.10	2.13
Fe–N2/O6	2.27	2.22	2.12	2.32	2.32	2.33	2.09	2.08

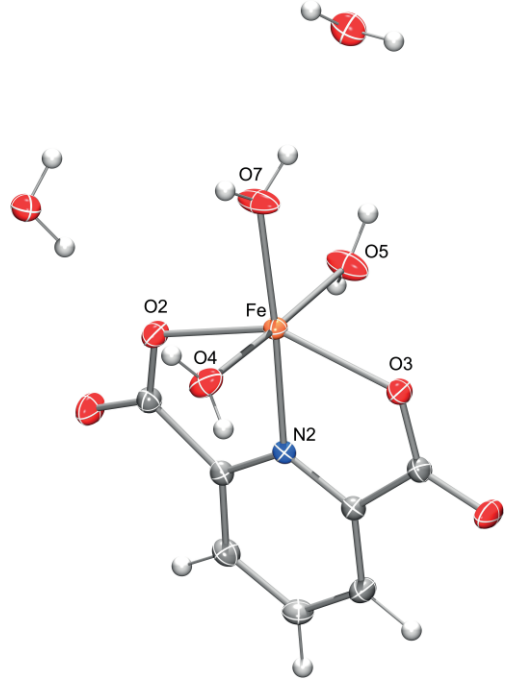

Figure 6. Nitrosyl-free [Fe(dipic)$(H_2O)_3$]·$2H_2O$ units in crystals of **3g**. Space group: $P2_12_12_1$. Thermal ellipsoids are drawn at 50 % probability.

On closer inspection of the X-ray diffraction results, two facts stand out: (1) All equatorial ligands are tilted away from the nitrosyl group. The mean NO–Fe–L_{eq} angle for all compounds **2** is 97.4°. This can also be observed for most other mono-nitrosyl–iron compounds (MNICs) known in the literature – for heme nitrosyl compounds[16] or the nitroprusside anion, amongst others.[17] Comparing **2g** with its direct nitrosyl-free homologue **3g** (in which an aqua ligand replaces nitric oxide, see Figure 6) shows that, while in **2g** the equatorial aqua ligands are tilted away from the nitrosyl group with 95.5 and 93.3° (see Figure 5), they are tilted towards the axial aqua ligand in **3g** (88°). The reason seems to be the steric demand of the orbital lobes of the Fe–NO π interaction, which is discussed below. (2) In all crystal structures of **2**, the nitrosyl oxygen atoms have large thermal ellipsoids, indicating a rather flat bending potential of the Fe–N–O moiety, which will also be discussed below.

IR and UV/Vis Spectroscopy

IR spectra were recorded for all solid compounds **2** by using the ATR technique (Table 2). The spectra show a single ν(NO) stretching vibration band in the range of 1764 (**2d**) to 1806 cm^{-1} (**2g**). UV/Vis spectra of solid samples of **2** show absorption bands around 340, 400, 460, 600 and 690 nm. Both IR and UV/Vis data match published results for octahedrally coordinated quartet-{FeNO}^{7} compounds.[15,18]

Table 2. IR and UV/Vis spectroscopic data for **2**.

Compound	ν(NO) /cm^{-1}	λ /nm				
2a	1772	340	414	459	618	692
2b	1782	341	402	457	625	691
2c	1799	340	407	459	571	693
2d	1764					
2e	1803	341	408	459	596	692
2f	1800	341	402	459	595	691
2g	1806					

SQUID Magnetometry

The magnetic properties of **2a** and **2e** were determined by SQUID magnetometry. Using Equation (1), the magnetic moment μ_{eff} was calculated from $\chi_M T$. The values obtained were compared with the spin-only value [$\mu_{s.o.}$, Equation (2)]. Figure 7 shows the result for **2a** and **2e**. Both compounds show nearly perfect Curie–Weiss behaviour, and the drop at low temperatures is probably due to zero-field splitting. Using Equation 1, μ_{eff} values of 3.95 and 4.13 μ_B were obtained for **2a** and **2e**, respectively. These values lie in the expected range for quartet compounds with a spin-only value of $\mu_{s.o.}$ = 3.88 μ_B.

$$\mu_{eff} = \sqrt{\frac{3k_B\chi_m T}{\mu_0 N_A \mu_B^2}} \quad (1)$$

$$\mu_{s.o.} = 2S(S+1) \quad (2)$$

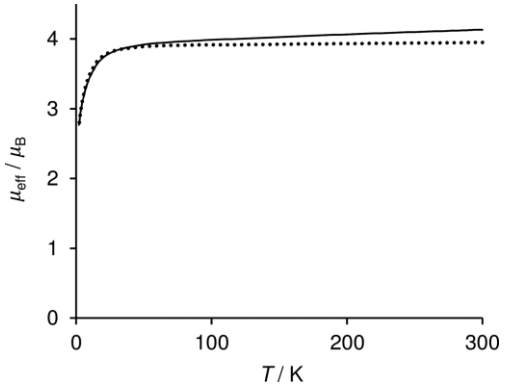

Figure 7. μ_{eff} vs. T plots for **2a** (solid line) and **2e** (dotted line).

Quantum-Chemical Calculations

We carried out quantum-chemical calculations based on the DFT and CASSCF methods to gain insight into the electronic properties of compounds **2**. In particular, we attempted to evaluate the oxidation state of the iron central atom and the nitrosyl ligand. Various theoretical and spectroscopic studies have been published on this issue. Most of them describe either a high-spin $Fe^{III}/^3NO^-$[9a,9c,10b,15b,18d,18e,18i,19] or a high-spin $Fe^{II}/^2NO$[10a,20] couple with antiferromagnetic Fe–NO coupling in both cases.

In terms of the X-ray-derived data for **2**, the best agreement between calculated and experimental data was achieved by using the def2-TZVP[21] basis set, the dispersion-corrected functional B97-D[22] and the D-COSMO-RS solvation model[23] to account for the hydrogen-bond network in the crystal structures. All calculations were performed by using spin-unrestricted open-shell systems with three unpaired electrons.

The electronic description of the Fe(NO) moiety is the same for all compounds **2** and is influenced minimally by the different chelating ligands. The Fe–NO interaction is dominated by the coupling of two spin-down NO π* orbitals with the symmetrically matching Fe d_{xz} and Fe d_{yz} spin-up orbitals (Figure 8, top-right, shows one of them). The orbitals possess 30 to 40 % Fe d character, up to 2 % Fe p character and 50 to 60 % NO π* character. The bonds are supported by energetically low-lying interactions of the NO π, 5σ and 4σ orbitals with corresponding Fe orbitals for both up- and down-spin electrons (for molecular orbitals of free NO see the Supporting Information). Only small Fe–NO antibonding contributions were detected, the most important one being that of the NO 5σ orbital. It interacts with the spin-up Fe d_{z^2} orbital, which is, in turn, antibonding with respect to the heteroatom *trans* to NO. This molecular orbital (MO) represents the HOMO and possesses a 25 to 35 % Fe d character and a 5 to 10 % NO character. The same interaction was found with lower energy and a bonding interaction between the Fe d_{z^2} orbital and the heteroatom *trans* to NO. Figure 8 illustrates the overlap population density of states (OPDOS) between Fe and NO of **2a** and relevant occupied MOs. It is representative for all compounds **2**.

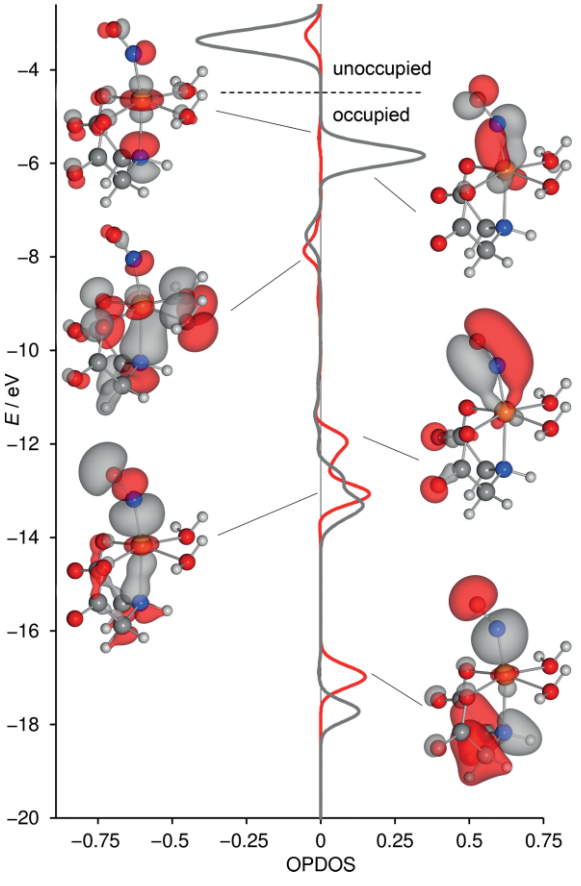

Figure 8. Plot of the overlap population density of states (OPDOS) between Fe and NO of **2a** together with relevant bonding and antibonding MOs.[27b] Spin-up OPDOS are in red, spin-down OPDOS are in grey.

In an alternative presentation style, following the usage in ref.,[19] the Fe–NO interaction is mapped in terms of the unoccupied counterparts of the occupied frontier orbitals. Figure 9 shows the seven relevant MOs: five unoccupied β-spin orbitals

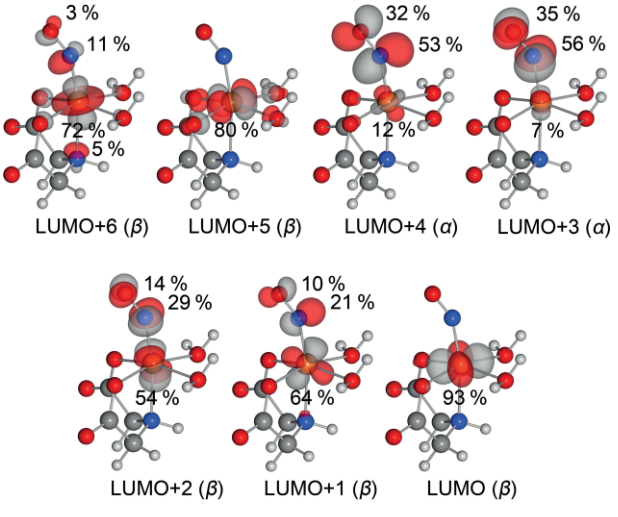

Figure 9. Contours of the seven most stable unoccupied orbitals. Individual contributions are derived from Mulliken population analyses.

and two α-spin MOs that highlight the significance of largely covalent π interactions including, to some extent, spin polarisation.

The orbital pictures suggest that Solomon's view on the Fe–NO bond – a $^3NO^-$ ligand, antiferromagnetically coupled to a high-spin Fe^{III} centre – may serve as a good starting point which, however, has to be modified by taking into account charge compensation due to largely covalent Fe–NO bonds.

Furthermore, this view is supported by a broken-symmetry approach. Using the Yamaguchi formula, coupling constants in the range of 2205 to 2318 cm^{-1} and overlap integrals S_{ab} between 0.82 and 0.84 were obtained for the compounds in this work – both parameters indicating largely, but not entirely, normal bonds in terms of bond energies and α/β overlap.[24]

Focussing on charges on the iron atom and the nitrosyl ligand, we performed a Mulliken population analysis (MPA),[25] a natural population analysis (NPA),[26] and AOMix-FO charge decomposition analyses (CDA)[27] using the fragments ^2NO and $Fe^{II}L$ (L = all ligands but NO) resulting in Fe-to-NO charge transfer values of –0.04 and –0.03 for the α and the β regime, respectively. In agreement with these small numbers, the population analyses resulted in an approximately neutral nitrosyl ligand and a spin density close to unity (Table 3).

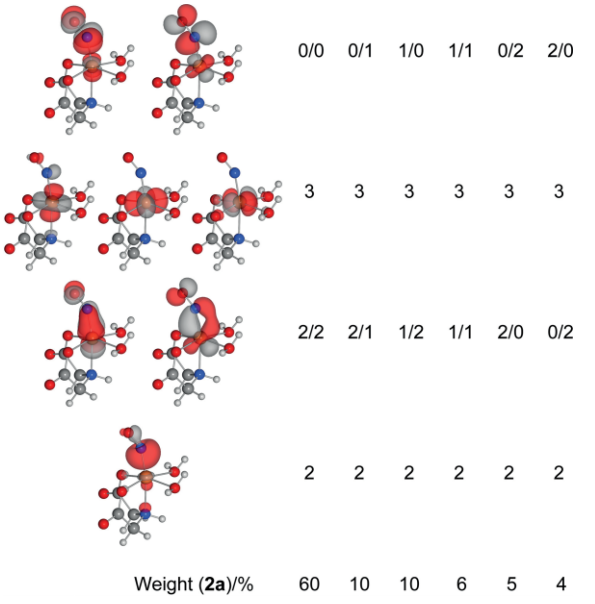

Figure 10. Active space in CASSCF calculations of **2a**. Given in the columns to the right of the orbitals is the number of electrons in these orbitals for each configuration state function. The weight of each configuration state function is given at the bottom of each column. Fe d double shells are omitted.

Table 3. MPA and NPA analysis on **2**. All values are elementary charges.

	Charge		Spin	
	Fe	NO	Fe	NO
MPA	0.57	0.07	3.57	–0.93
NPA	1.35	–0.06	3.51	–0.91

Table 4. Mulliken analysis on the CASSCF calculations of **2a**. All values are elementary charges.

	Fe	NO
Charge	1.12	–0.03
Spin	3.49	–0.55

In addition to the DFT calculations, CASSCF calculations for **2a** with an active space of 9 electrons in 13 orbitals were performed. Figure 10 shows the relevant natural orbitals representing the active space for **2a** and their occupations. The dominant configuration of the CAS wave function corresponds to the DFT result. The bonding interactions of the NO π^* orbitals with Fe d orbitals are occupied by two electrons each, and the remaining Fe d orbitals are occupied by one unpaired electron each. This configuration accounts for a 60 % weight of the complete active space wave function. A 35 % weight is distributed over different configurations, exciting electrons from the Fe–NO π bond into the Fe–NO π antibonding orbitals. This strong contribution of excited states is also reflected in the occupation numbers: the Fe–NO π bonding orbitals are occupied by 1.71 electrons, whereas their antibonding counterparts are occupied by 0.28 electrons. The remaining 5 % weight is attributed to excitations from the Fe–NO σ bond or into the Fe d double shells. Mulliken population analyses were performed again. As shown in Table 4, the CASSCF calculation assigns a more positive charge to the iron atom than the DFT calculations do (compare Table 3), but leaving the charge on the nitrosyl ligand as 0. The spin densities on the nitrosyl ligand and the iron atom are reduced as compared with those of the DFT calculations. The nitrosyl ligand now carries a β spin density of –0.55, and the iron atom carries an α spin density of +3.5.

In a different approach to analyse the results of the CASSCF calculations, the orbitals of the active space were localised to yield 10 iron orbitals and 3 NO orbitals. The oxidation state of each configuration-state function was taken as the sum of the occupied localised orbitals.[10c,28] The interpretation is fairly simple: with 66 % the dominant oxidation state of the iron atom is +II. The oxidation state +III accounts for 25 %, and the remaining 9 % corresponds to the oxidation state +I.

Comparison with Nitrosyl-Free Analogues

For some of the compounds **2** the corresponding nitrosyl-free Fe^{II} complexes, with an aqua ligand instead of the NO group, were synthesised. Others can be found in the literature together with the corresponding Fe^{III} complexes. The computational results may thus be supplemented on the basis of a simple atomic-distance argument (Table 5).

Comparing the experimental iron–ligand atomic distances shows that nitrosyl compounds **2** lie between the Fe^{II} and Fe^{III} complexes, but closer to the former. For **2g**, all three complexes share the same environment and ligands. Thus, it is particularly significant to observe that the parameters of the nitrosyl complex are close to those of Fe^{II}.

Taking all the results together, the Fe–NO interaction can be described as follows: the two NO π^* orbitals contribute spin-

Table 5. Comparison of crystal structures of compounds **2c** and **2g** with their corresponding nitrosyl-free Fe^{2+} and Fe^{3+} complexes. Distances are given in nm. The bond lengths denoted are the mean values of Fe–OAc or Fe–OH_2 bond lengths.

Compound	Fe–OAc	Fe–OH_2
$[\{Fe^{II}(H_2O)_2(oda)\}_n]$[29]	214	215
$[Fe(NO)(H_2O)_2(oda)]$ (**2c**)	207	208
$[Fe^{III}Cl(H_2O)_2(oda)]$[30]	200	203
$[Fe^{II}(dipic)(H_2O)_3]$ (**3g**)	216	212
$[Fe(dipic)(NO)(H_2O)_2]$ (**2g**)	212	211
$[Fe^{III}(dipic)(H_2O)_3]^+$[31]	201	200

down electrons to an overall quartet state of the high-spin {FeNO}^{7} moiety. Due to the strongly covalent character of the Fe–NO π interaction, spin-down electron density is transferred, to a large extent, onto the iron atom. As a result, population analyses calculate a divalent central metal atom bonded to a neutral NO ligand.

The Fe–N–O Angle

The Fe–N–O bond angle of high-spin {FeNO}^{7} complexes has been investigated as a particularly intriguing parameter in recent computational approaches, most notably in studies by Conradie and Ghosh.[6,10d,20a,32] With angles between 148° (**2d**) and 171° (**2b**), compounds **2** cover nearly the full range determined for quartet-{FeNO}^{7} compounds so far. Yet the coordination sphere of the iron atom is nearly the same for all compounds: all but **2c** feature an NO_4 coordination, and, in all but **2d**, the nitrosyl ligand coordinates *trans* to the central heteroatom of the chelating ligand.

In order to classify the now available experimental values, we performed DFT-based relaxed scans (Figure 11) on **2a**, **2c**, **2e** and **2g**. It became obvious that all compounds showed very flat Fe–N–O bending potentials. For 180°, the potentials were close to their minimum. On bending, the potentials stayed below 5 kJ mol^{-1} until the angle reached the range of 140° to 130°. MPA and NPA analyses showed no significant change of charge or spin population while bending the Fe–N–O moiety. Figure 12 shows a Walsh diagram of **2a** together with NPA analyses. At 180°, the HOMO is the σ antibonding interaction between the Fe d_{z^2} orbital and the 5 σ orbital of NO. On bending to 110°, the former HOMO is lowered in energy by 0.3 eV and becomes HOMO–2, a weak σ bonding interaction between the Fe d_{z^2} orbital and an NO π* orbital. Meanwhile HOMO–1 and

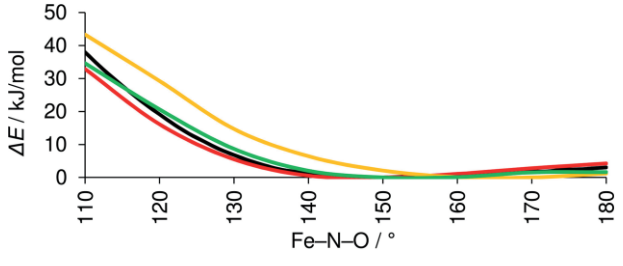

Figure 11. Fe–N–O bending potentials. At the 110° abscissa value, the energies increase in the order **2e**, **2d**, **2a**, **2g**.

HOMO–2, as bonding π interactions of the NO π* orbitals with the Fe d_{xz} and Fe d_{yz} orbitals, rise in energy by 0.5 eV. HOMO–1 also becomes a σ bond between the Fe d_{xz} orbital and an NO π* orbital, whereas HOMO–2 does not change at all except for the bending, and is now the HOMO.

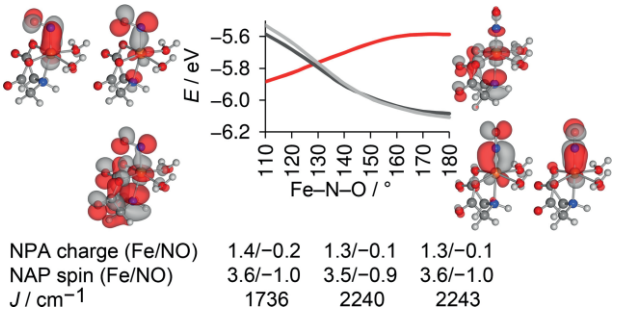

Figure 12. Walsh diagram of **2a**. Spin-up MOs are in red, spin-down MOs are in light and dark grey. Charge and spin are denoted for 110°, 144° and 180°. *J* is the coupling constant as derived from broken-symmetry calculations.

Hence, the flat bending potential is a result of counterbalanced bonding components over a significant angle range: (1) the in-plane (with *xz* as the reference plane) Fe–d_{xz}–NO–π* interaction, which is of the π type close to linearity of the FeNO moiety; on strong bending, this nitrosyl MO is part of a σ-type bond to a d_{z^2} atomic orbital of Fe; (2) the second component, the out-of-the-FeNO-plane π bond, which shows little dependence between the bond angle and orbital overlap; (3) the repulsive, σ-antibonding interaction of the NO 5σ lone pair with the Fe d_{z^2} orbital, which is minimised on bending. Experimentally, the flat potential was mirrored by the large thermal ellipsoids of the nitrosyl oxygen atoms.

As a result, the actual Fe–N–O angle reflects the discussed subtle electronic effects, but also the intermolecular interactions and crystal packing effects which, in total, determine the experimentally found position on the potential-energy curve.

Conclusions

We have presented crystal structures of seven quartet-{FeNO}^{7} compounds with iminodiacetate derivatives as chelating ligands. With respect to a simple stability criterion (NO loss upon purging with Ar or N_2), they all belong to a class of less stable derivatives of this type, as does the parent compound of this chemistry, the $[Fe(H_2O)_5(NO)]^{2+}$ aqua species. Notably, the oda derivative shares the O_5 donor set (and the low stability) with the parent aqua complex.

Structurally, the compounds feature slightly bent (nitrosyl)iron moieties with Fe–N–O angles between 148° and 171°. In IR spectra, the ν(NO) stretching vibration bands lie between 1764 cm^{-1} and 1814 cm^{-1}. The Fe–N–O angle is characterised by a flat bending potential, which is the result of opposing contributions to the Fe–NO interaction: the two Fe–NO π bonds and the three-electron situation in the Fe–NO σ bonding/antibonding couple. By DFT and CASSCF calculations, and by comparing the compounds **2** with nitrosyl-free Fe^{II} and Fe^{III} com-

pounds, we showed that the Fe–NO interaction in these less stable quartet-{FeNO}^{7} compounds is adequately described as a mostly covalent, slightly spin-polarised Fe–NO interaction with an approximately zero net charge on the nitrosyl ligand. This preliminary result is placed on a broader experimental basis in the accompanying work[13] that deals with stable representatives of {FeNO}^{7}-type complexes. By comparison, one structural feature remains constant throughout the members of both subclasses, namely their hexacoordination independent of the various co-ligands. For the ligands with a limited denticity (this work), aqua ligands fill up the coordination octahedron, whereas dangling functions preserve hexacoordination with the multidentate co-ligands of the stable subclass.

Experimental Section

General Remarks

IR Spectroscopy: IR spectra were recorded with a Jasco FT/IR-460 Plus spectrometer. Solid samples were recorded using an ATR diamond plate. All spectra were interpreted with the software Spectra Manager 2.07.00. All signals are given in wavenumbers.

UV/Vis Spectroscopy: UV/Vis spectra of solid samples were measured with a Cary 500 Scan UV/Vis/NIR-Spectrophotometer with a Labsphere DRA-CA-5500 photometer sphere. The diffuse reflection was measured and converted by using the Kubelka–Munk function.[33]

X-ray Diffraction

Crystals were selected by using a Leica MZ6 polarisation microscope. Suitable crystals were measured with single-crystal diffractometers of the types Bruker Nonius Kappa CCD, Bruker D8 Quest and Bruker D8 Venture using Mo-K_α irradiation. The structure solutions were carried out by direct methods using SHELXS-2014.[34] The structures were refined by full-matrix least-squares calculations on F^2 using SHELXL-2014 and ShelXLe.[35] Distances and angles were calculated with Platon.[36] For visualisation, the programs ORTEP and POV-Ray were used.[37]

CCDC 1510832 (for **2b**), 1510833 (for **2a**), 1510834 (for **2e**), 1510835 (for **2d**), 1510836 (for **2c**), 1510837 (for **2f**), 1510838 (for **2g**) and 1510839 (for **3g**) contain the supplementary crystallographic data for this paper. These data can be obtained free of charge from The Cambridge Crystallographic Data Centre.

Magnetic Susceptibilities: Magnetic susceptibility data were collected with a Quantum Design MPMS XL-5 SQUID magnetometer over 10–300 K in the sweep mode. All samples were placed in gelatine capsules held within plastic straws. The data were corrected for the diamagnetic magnetisation of the ligands, which were estimated using Pascal's constants, and for the sample holder.[38]

Computational Methods: All quantum-chemical calculations at the DFT level were performed with the program system Turbomole.[39] Initial geometries were taken either from crystal-structure analyses or set up using TmoleX.[40] Wave functions were calculated at the multipole-accelerated RI-DFT level using def2-TZVP basis sets and the functionals BP-86, B97-D and TPSSh.[21,22,41] Dispersion correction was applied by using Grimme's DFT-D3 with BJ-damping.[42] D-COSMO-RS was used to simulate hydrogen-bond networks.[23] Frequency analyses were done numerically. CASSCF calculations were carried out with the ORCA program system.[43]

Synthesis of Quartet-{FeNO}^{7} Compounds

All reactions involving iron compounds were carried out under an argon atmosphere using standard Schlenk techniques and degassed solvents. Pipettes, syringes and cannulas, used for dosing the solvents, were flushed three times with argon before usage. Water and acetone were degassed by refluxing while bubbling argon through them and were stored in Schlenk flasks under an argon atmosphere. Nitric oxide was purchased from Air Liquide and was purified by bubbling through a sodium hydroxide solution (4 M) directly prior to use. Excess nitric oxide was eliminated by bubbling through a saturated sulfamic acid solution. $FeSO_4{\cdot}7H_2O$ and the chelating ligands H_2ida, H_2heida, H_2oda, H_2bnida and H_2dipic were purchased from Sigma-Aldrich, Acros or Grüssing. H_2phida and H_2brbnida were synthesised according to literature procedures.[44]

In one chamber of a two-chamber Schlenk flask $FeSO_4{\cdot}7H_2O$ (278 mg, 1.0 mmol) and the desired chelating ligand (1.0 mmol) were dissolved in water (5 mL), forming a colourless solution. Nitric oxide was bubbled through the solution for 10 min, turning it dark green. The gas phase of the Schlenk flask was flushed with argon, and acetone (5 mL) was filled into the empty chamber of the Schlenk flask to induce crystallisation. After one to eight weeks, **2** was obtained as green crystals.

[Fe(ida)(NO)(OH$_2$)$_2$] (2a): Yield 63 mg (25 %). IR (solid, ATR): $\tilde{\nu}$ = 1772(s), 1566(vs), 1454(s), 1408(s), 1338(m), 1317(m), 1256(m), 1208(w), 1143(m), 950(m), 922(s), 797(s), 723(m), 659(m) cm^{-1}. UV/Vis (solid): λ = 340, 414, 459, 618, 692 nm.

[Fe(heida)(NO)(OH$_2$)] (2b): Yield 75 mg (27 %). IR (solid, ATR): $\tilde{\nu}$ = 1782(m), 1555(vs), 1480(m), 1444(m), 1428(m), 1401(s), 1388(s), 1380(s), 1351(s), 1323(m), 1300(vs), 1264(m), 1253(m), 1221(w), 1155(w), 1108(w), 1066(m), 1055(m), 998(s), 973(w), 921(s), 883(s), 839(s), 812(vs), 737(s), 695(m), 686(m), 659(m) cm^{-1}. UV/Vis (solid): λ = 341, 402, 457, 625, 691 nm.

[Fe(NO)(OH$_2$)$_2$(oda)] (2c): Yield 53 mg (21 %). IR (solid, ATR): $\tilde{\nu}$ = 1799(m), 1557(vs), 1467(m), 1419(vs), 1352(m), 1305(s), 1133(s), 1034(m), 933(m), 806(m), 796(m), 729(s), 677(m) cm^{-1}. UV/Vis (solid): λ = 340, 407, 459, 571, 693 nm.

[Fe(NO)(OH$_2$)$_2$(phida)]·H$_2$O (2d): Yield 140 mg (40 %). IR (solid, ATR): $\tilde{\nu}$ = 1763(s), 1680(w), 1573(vs), 1496(s), 1454(w), 1397(s), 1295(s), 1196(m), 1143(m), 1028(w), 976(m), 919(m), 892(w), 773(s), 759(s), 690(vs) cm^{-1}.

[Fe(bnida)(NO)(OH$_2$)$_2$] (2e): Yield 51 mg (15 %). IR (solid, ATR): $\tilde{\nu}$ = 1790(m), 1606(s), 1494(w), 1456(w), 1394(m), 1337(m), 1219(w), 1200(w), 1090(w), 1075(m), 943(m), 905(m), 763(s), 703(s) cm^{-1}. UV/Vis (solid): λ = 341, 408, 459, 596, 692 nm.

[Fe(brbnida)(NO)(OH$_2$)$_2$] (2f): Yield 55 mg (13 %). IR (solid, ATR): $\tilde{\nu}$ = 1800(m), 1604(vs), 1486(w), 1464(w), 1438(vw), 1398(s), 1367(m), 1342(m), 1313(w), 1292(w), 1219(w), 1089(w), 1071(w), 1011(w), 975(vw), 956(vw), 938(m), 910(m), 850(m), 797(m), 766(w), 748(w), 720(m) cm^{-1}. UV/Vis (solid): λ = 371, 402, 459, 595, 691 nm.

[Fe(dipic)(NO)(OH$_2$)$_2$] (2g): Yield 109 mg (38 %). IR (solid, ATR): $\tilde{\nu}$ = 1814(s), 1640(s), 1607(s), 1592(s), 1574(s), 1431(m), 1375(s), 1359(s), 1278(s), 1184(m), 1154(w), 1082(m), 1036(w), 1004(w), 920(s), 839(w), 814(w), 769(vs), 750(vs), 688(vs), 668(vs) cm^{-1}.

Acknowledgments

The authors gratefully acknowledge financial support from the Deutsche Forschungsgemeinschaft (DFG) priority program SPP1740, aimed at the "influence of local transport processes in chemical reactions in bubble flows".

Keywords: Iron · Nitrosyl ligands · Coordination modes · Density functional calculations · Structure elucidation

[1] a) V. Kohlschütter, M. Kutscheroff, *Ber. Dtsch. Chem. Ges.* **1904**, *37*, 3044–3052; b) W. Manchot, K. Zechentmayer, *Justus Liebigs Ann. Chem.* **1906**, *350*, 368–389; c) V. Kohlschütter, M. Kutscheroff, *Ber. Dtsch. Chem. Ges.* **1907**, *40*, 873–878; d) W. Manchot, F. Huttner, *Justus Liebigs Ann. Chem.* **1910**, *372*, 153–178.
[2] W. P. Griffith, J. Lewis, G. Wilkinson, *J. Chem. Soc.* **1958**, 3993–3998.
[3] a) H. I. Schlesinger, A. Salathe, *J. Am. Chem. Soc.* **1923**, *45*, 1863–1878; b) W. Manchot, E. Linckh, *Ber. Dtsch. Chem. Ges.* **1926**, *59*, 406–411.
[4] N. G. Connelly, C. Gardner, *J. Chem. Soc., Dalton Trans.* **1976**, 1525–1527.
[5] J. H. Enemark, R. D. Feltham, *Coord. Chem. Rev.* **1974**, *13*, 339–406.
[6] J. Conradie, K. H. Hopmann, A. Ghosh, *J. Phys. Chem. B* **2010**, *114*, 8517–8524.
[7] D. Littlejohn, S. G. Chang, *Ind. Eng. Chem. Res.* **1987**, *26*, 1232–1234.
[8] a) T. Schneppensieper, S. Finkler, A. Czap, R. van Eldik, M. Heus, P. Nieuwenhuizen, C. Wreesmann, W. Abma, *Eur. J. Inorg. Chem.* **2001**, 491–501; b) T. Schneppensieper, A. Wanat, G. Stochel, S. Goldstein, D. Meyerstein, R. van Eldik, *Eur. J. Inorg. Chem.* **2001**, 2317–2325; c) T. Schneppensieper, A. Wanat, G. Stochel, R. van Eldik, *Inorg. Chem.* **2002**, *41*, 2565–2573.
[9] a) Y. Zhang, M. A. Pavlosky, C. A. Brown, T. E. Westre, B. Hedman, K. O. Hodgson, E. I. Solomon, *J. Am. Chem. Soc.* **1992**, *114*, 9189–9191; b) T. E. Westre, A. di Cicco, A. Filipponi, C. R. Natoli, B. Hedman, E. I. Solomon, K. O. Hodgson, *J. Am. Chem. Soc.* **1994**, *116*, 6757–6768; c) C. A. Brown, M. A. Pavlosky, T. E. Westre, Y. Zhang, B. Hedman, K. O. Hodgson, E. I. Solomon, *J. Am. Chem. Soc.* **1995**, *117*, 715–732.
[10] a) H.-Y. Cheng, S. Chang, P.-Y. Tsai, *J. Phys. Chem. A* **2004**, *108*, 358–361; b) A. Wanat, T. Schneppensieper, G. Stochel, R. van Eldik, E. Bill, K. Wieghardt, *Inorg. Chem.* **2002**, *41*, 4–10; c) M. Radón, E. Broclawik, K. Pierloot, *J. Phys. Chem. B* **2010**, *114*, 1518–1528; d) J. Conradie, A. Ghosh, *Inorg. Chem.* **2011**, *50*, 4223–4225; e) E. Broclawik, A. Stępniewski, M. Radoń, *J. Inorg. Biochem.* **2014**, *136*, 147–153.
[11] T. C. Berto, A. L. Speelman, S. Zheng, N. Lehnert, *Coord. Chem. Rev.* **2013**, *257*, 244–259.
[12] J. McCracken, P. J. Cappillino, J. S. McNally, M. D. Krzyaniak, M. Howart, P. C. Tarves, J. P. Caradonna, *Inorg. Chem.* **2015**, *54*, 6486–6497.
[13] B. M. Aas, P. Klüfers, *Eur. J. Inorg. Chem.* **2017**, 2313–2320.
[14] T. Woike, D. Schaniel, unpublished.
[15] a) Y.-M. Chiou, L. Que Jr., *Inorg. Chem.* **1995**, *34*, 3270–3278; b) T. C. Berto, M. B. Hoffman, Y. Murata, K. B. Landenberger, E. E. Alp, J. Zhao, N. Lehnert, *J. Am. Chem. Soc.* **2011**, *133*, 16714–16717; c) A. Majumdar, S. J. Lippard, *Inorg. Chem.* **2013**, *52*, 13292–13294; d) J. Li, A. Banerjee, P. L. Pawlak, W. W. Brennessel, F. A. Chavez, *Inorg. Chem.* **2014**, *53*, 5414–5416; e) E. Victor, S. Kim, S. J. Lippard, *Inorg. Chem.* **2014**, *53*, 12809–12821; f) E. Victor, M. A. Minier, S. J. Lippard, *Eur. J. Inorg. Chem.* **2014**, 5640–5645.
[16] N. J. Silvernail, J. W. Pavlik, B. C. Noll, C. E. Schulz, W. R. Scheidt, *Inorg. Chem.* **2008**, *47*, 912–920.
[17] E. Wenger, S. Dahaoui, P. Alle, P. Parois, C. Palin, C. Lecomte, D. Schaniel, *Acta Crystallogr., Sect. B: Struct. Sci.* **2014**, *70*, 783–791.
[18] a) K. Pohl, K. Wieghardt, B. Nuber, J. Weiss, *J. Chem. Soc., Dalton Trans.* **1987**, 187–192; b) C. R. Randall, Y. Zang, A. E. True, L. Que Jr., J. M. Charnock, C. D. Garner, Y. Fujishima, C. J. Schofield, J. E. Baldwin, *Biochemistry* **1993**, *32*, 6664–6673; c) A. L. Feig, M. T. Bautista, S. J. Lippard, *Inorg. Chem.* **1996**, *35*, 6892–6898; d) C. Hauser, T. Glaser, E. Bill, T. Weyhermüller, K. Wieghardt, *J. Am. Chem. Soc.* **2000**, *122*, 4352–4365; e) M. Li, D. Bonnet, E. Bill, F. Neese, T. Weyhermüller, N. Blum, D. Sellmann, K. Wieghardt, *Inorg. Chem.* **2002**, *41*, 3444–3456; f) B. Weber, H. Görls, M. Rudolph, E.-G. Jäger, *Inorg. Chim. Acta* **2002**, *337*, 247–265; g) D. P. Klein, V. G. Young Jr., W. B. Tolman, L. Que Jr., *Inorg. Chem.* **2006**, *45*, 8006–8008; h) F.-T. Tsai, P.-L. Chen, W.-F. Liaw, *J. Am. Chem. Soc.* **2010**, *132*, 5290–5299; i) G. Villar-Acevedo, E. Nam, S. Fitch, J. Benedict, J. Freudenthal, W. Kaminsky, J. a. Kovacs, *J. Am. Chem. Soc.* **2011**, *133*, 1419–1427; j) H. Park, M. M. Bittner, J. S. Baus, S. V. Lindeman, A. T. Fiedler, *Inorg. Chem.* **2012**, *51*, 10279–10289; k) F.-T. Tsai, Y.-C. Lee, M.-H. Chiang, W.-F. Liaw, *Inorg. Chem.* **2013**, *52*, 464–473; l) S. Zheng, T. C. Berto, E. W. Dahl, M. B. Hoffman, A. L. Speelman, N. Lehnert, *J. Am. Chem. Soc.* **2013**, *135*, 4902–4905.
[19] a) G. Schenk, M. Y. M. Pau, E. I. Solomon, *J. Am. Chem. Soc.* **2004**, *126*, 505–515; b) C. D. Brown, M. L. Neidig, M. B. Neibergall, J. D. Lipscomb, E. I. Solomon, *J. Am. Chem. Soc.* **2007**, *129*, 7427–7438; c) A. R. Diebold, C. D. Brown-Marshall, M. L. Neidig, J. M. Brownlee, G. R. Moran, E. I. Solomon, *J. Am. Chem. Soc.* **2011**, *133*, 18148–18160; d) N. Sun, L. V. Liu, A. Dey, G. Villar-Acevedo, J. a. Kovacs, M. Y. Darensbourg, K. O. Hodgson, B. Hedman, E. I. Solomon, *Inorg. Chem.* **2011**, *50*, 427–436; e) A. Earnshaw, E. A. King, L. F. Larkworthy, *J. Chem. Soc. A* **1969**, 2459–2463; f) H. Twilfer, F.-H. Bernhardt, K. Gersonde, *Eur. J. Biochem.* **1985**, *147*, 171–176; g) T. A. Jackson, E. Yikilmaz, A.-F. Miller, T. C. Brunold, *J. Am. Chem. Soc.* **2003**, *125*, 8348–8363; h) K. H. Hopmann, A. Ghosh, L. Noodleman, *Inorg. Chem.* **2009**, *48*, 9155–9165; i) S. Ye, J. C. Price, E. W. Barr, M. T. Green, J. M. Bollinger, C. Krebs, F. Neese, *J. Am. Chem. Soc.* **2010**, *132*, 4739–4751.
[20] a) J. Conradie, D. a. Quarless, H.-F. Hsu, T. C. Harrop, S. J. Lippard, S. a. Koch, A. Ghosh, *J. Am. Chem. Soc.* **2007**, *129*, 10446–10456; b) J. C. Salerno, J. N. Siedow, *Biochim. Biophys. Acta Protein Struct.* **1979**, *579*, 246–251; c) D. M. Arciero, J. D. Lipscomb, B. H. Huynh, T. A. Kent, M. Eckard, *J. Biol. Chem.* **1983**, *258*, 14981–14991; d) Y. Zhang, E. Oldfield, *J. Phys. Chem. A* **2003**, *107*, 4147–4150; e) Y. Zhang, E. Oldfield, *J. Am. Chem. Soc.* **2004**, *126*, 9494–9495; f) H.-Y. Cheng, S. Chang, *Int. J. Quantum Chem.* **2005**, *105*, 511–517; g) S. Chakraborty, J. Reed, M. Ross, M. J. Nilges, I. D. Petrik, S. Ghosh, S. Hammes-Schiffer, J. T. Sage, Y. Zhang, C. E. Schulz, Y. Lu, *Angew. Chem. Int. Ed.* **2014**, *53*, 2417–2421; *Angew. Chem.* **2014**, *126*, 2449.
[21] F. Weigend, R. Ahlrichs, *Phys. Chem. Chem. Phys.* **2005**, *7*, 3297–3305.
[22] S. Grimme, *J. Comput. Chem.* **2006**, *27*, 1787–1799.
[23] a) S. Sinnecker, A. Rajendran, A. Klamt, M. Diedenhofen, F. Neese, *J. Phys. Chem. A* **2006**, *110*, 2235–2245; b) A. Klamt, M. Diedenhofen, *J. Phys. Chem. A* **2015**, *119*, 5439–5445.
[24] T. Soda, Y. Kitagawa, T. Onishi, Y. Takano, Y. Shigeta, H. Nagao, Y. Yoshioka, K. Yamaguchi, *Chem. Phys. Lett.* **2000**, *319*, 223–230.
[25] R. S. Mulliken, *J. Chem. Phys.* **1955**, *23*, 1833–1840.
[26] A. E. Reed, R. B. Weinstock, F. Weinhold, *J. Chem. Phys.* **1985**, *83*, 735–746.
[27] a) S. I. Gorelsky, A. B. P. Lever, *J. Organomet. Chem.* **2001**, *635*, 187–196; b) S. I. Gorelsky, *AOMix 2.8*: Program for Molecular Orbital Analysis, **1997–2013**.
[28] B. O. Roos, V. Veryazov, J. Conradie, P. R. Taylor, A. Ghosh, *J. Phys. Chem. B* **2008**, *112*, 14099–14102.
[29] A. Grirrane, A. Pastor, C. Mealli, A. Ienco, P. Rosa, R. Prado-Gotor, A. Galindo, *Inorg. Chim. Acta* **2004**, *357*, 4215–4219.
[30] A. K. Powell, J. M. Charnock, A. C. Flood, C. D. Garner, M. J. Ware, W. Clegg, *J. Chem. Soc., Dalton Trans.* **1992**, 203–207.
[31] K. A. Abboud, C. Xu, R. S. Drago, *Acta Crystallogr., Sect. C: Cryst. Struct. Commun.* **1998**, *54*, 1270–1273.
[32] J. Conradie, A. Ghosh, *J. Inorg. Biochem.* **2006**, *100*, 2069–2073.
[33] G. Kortüm, *Reflexionsspektroskopie*, Springer, Berlin, Heidelberg, **1969**, pp. 725–727.
[34] G. M. Sheldrick, *Acta Crystallogr., Sect. A: Found. Crystallogr.* **2008**, *64*, 112–122.
[35] a) G. M. Sheldrick, *Acta Crystallogr., Sect. C: Struct. Chem.* **2015**, *71*, 3–8; b) C. B. Hübschle, G. M. Sheldrick, B. Dittrich, *J. Appl. Crystallogr.* **2011**, *44*, 1281–1284.
[36] A. L. Spek, *Acta Crystallogr., Sect. D: Biol. Crystallogr.* **2009**, *65*, 148–155.
[37] a) L. J. Farrugia, *J. Appl. Crystallogr.* **2012**, *45*, 849–854; b) *Persistence of Vision Raytracer* (version 3.6), Persistence of Vision Pty. Ltd., **2004**, retrieved from http://www.povray.org/download/.
[38] G. A. Bain, J. F. Berry, *J. Chem. Educ.* **2008**, *85*, 532–536.
[39] a) TURBOMOLE V6.6 **2014**, a development of University of Karlsruhe and Forschungszentrum Karlsruhe GmbH, 1989–2007, TURBOMOLE GmbH, since 2007; available from http://www.turbomole.com; b) R. Ahlrichs, M. Bär, M. Häser, H. Horn, C. Kölmel, *Chem. Phys. Lett.* **1989**, *162*, 165–169.
[40] C. Steffen, K. Thomas, U. Huniar, A. Hellweg, O. Rubner, A. Schroer, *J. Comput. Chem.* **2010**, *31*, 2967–2970.
[41] a) O. Treutler, R. Ahlrichs, *J. Chem. Phys.* **1995**, *102*, 346–354; b) M. Sierka, A. Hogekamp, R. Ahlrichs, *J. Chem. Phys.* **2003**, *118*, 9136–9148; c) K. Eichkorn, F. Weigend, O. Treutler, R. Ahlrichs, *Theor. Chem. Acc.* **1997**, *97*, 119–124; d) F. Weigend, *Phys. Chem. Chem. Phys.* **2006**, *8*, 1057–1065; e) A. D. Becke, *Phys. Rev. A* **1988**, *38*, 3098–3100; f) J. P. Perdew, *Phys. Rev. B* **1986**, *33*, 8822–8824; g) J. P. Perdew, Y. Wang, *Phys. Rev. B* **1992**, *45*,

13244–13249; h) J. Tao, J. P. Perdew, V. N. Staroverov, G. E. Scuseria, *Phys. Rev. Lett.* **2003**, *91*, 1464011–1464014; i) V. N. Staroverov, G. E. Scuseria, J. Tao, J. P. Perdew, *J. Chem. Phys.* **2003**, *119*, 12129–12137.

[42] S. Grimme, J. Antony, S. Ehrlich, H. Krieg, *J. Chem. Phys.* **2010**, *132*, 15410401–15410419.

[43] F. Neese, *Wiley Interdiscip. Rev.: Comput. Mol. Sci.* **2012**, *2*, 73–78.

[44] a) I. R. Gould, J. R. Lenhard, S. Farid, *J. Phys. Chem. A* **2004**, *108*, 10949–10956; b) N. Smrečki, B.-M. Kukovec, M. Đaković, Z. Popović, *Inorg. Chim. Acta* **2013**, *400*, 122–129.

Received: November 4, 2016